

Stimulated Surface-Plasma-Wave Scattering and Growth of a Periodic Structure in Laser-Photodeposited Metal Films

S. R. J. Brueck and D. J. Ehrlich

Lincoln Laboratory, Massachusetts Institute of Technology, Lexington, Massachusetts 02173

(Received 5 March 1982)

Ripple morphologies of submicrometer spatial period are observed on metal films grown by UV laser photolysis of adsorbed organometallic molecules. This structure develops from surface roughness by coupling of the incident UV field to a surface-plasma wave. The intensity variation due to interference between the incident laser field and the surface-plasma wave modulates the film growth rate which in turn enhances the scattering of the incident field into the surface-plasma wave; an exponentially growing instability results.

PACS numbers: 68.55.+b, 71.45.Gm, 78.65.Jd

In this Letter we demonstrate that surface-plasma-wave¹ (SPW) effects result in the growth of high spatial frequency surface relief in thin photochemically deposited metal films. Initially a weak SPW is excited by surface-roughness-induced scattering from the incident field; the spatial modulation of the optical intensity resulting from the interference between the incident wave and the SPW promotes the growth of a periodic (ripple) structure which increases the scattering into the SPW. There is a positive gain coefficient increasing both the film structure and SPW intensity for spatial frequencies ranging from approximately the incident-light wave vector to the SPW wave vector. This results in exponential growth of a periodic structure exhibiting this range of wave vectors. The process is somewhat analogous to stimulated Raman scattering where the grating structure plays the role of the material excitation and the SPW corresponds to the Stokes beam.

Surface-plasma-wave effects on grating structures were first observed by Wood.² More recently, coupling to SPW's has been shown^{3,4} to result in substantial field enhancements in the vicinity of a metal/dielectric interface and consequently to provide heightened sensitivity for various linear and nonlinear optical spectroscopic studies of the interface. This work is the first demonstration of an exponentially growing instability involving surface electromagnetic waves.

Specifically, we have observed these effects in the laser photochemical deposition of Cd, Zn, and Al films. As described previously,^{5,6} the films are deposited by UV laser photolysis of organometallic molecular gases near a substrate surface. A microwatt power-level, cw, UV laser source, obtained by frequency doubling of the out-

put of a 514.5-nm Ar-ion laser, is focused (1–100 μm diam) to moderate intensity levels ($< 10 \text{ W/cm}^2$) on the Si or SiO_2 substrate surface in the presence of a low-pressure (~ 1 Torr) organometallic gas [$\text{Cd}(\text{CH}_3)_2$, $\text{Zn}(\text{CH}_3)_2$, or $\text{Al}_2(\text{CH}_3)_6$]. Film growth proceeds at a rate of 0.1–1 nm/s by linear photochemical dissociation of the organometallic molecules and condensation of the free metal atoms. Laser heating of the 300-K substrates is less than 1 K.

For these wavelength and pressure conditions, photodeposition occurs primarily⁶ by photolysis of the van der Waals molecular films on the substrate surface. Scanning electron micrographs (SEM) of a typical Cd film are shown in Fig. 1. A comparison of the SEM's for the two observation angles of 60° [Fig. 1(a)] and normal incidence [Fig. 1(b)] shows that, although a ripple structure appears in two directions, the dominant structure is aligned approximately perpendicular to the laser polarization direction. Rotation of the laser

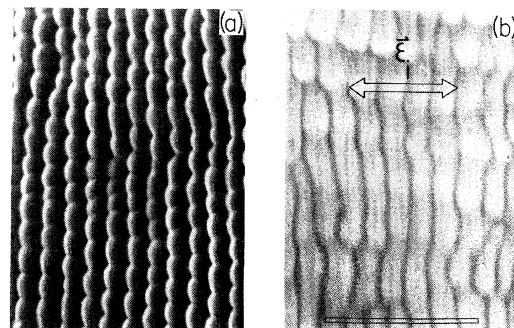


FIG. 1. SEM's of ripple structure in a ~ 200 -nm-thick photodeposited Cd film on a SiO_2 substrate at viewing angles of (a) 60° , and (b) normal incidence. A $1\text{-}\mu\text{m}$ scale (horizontal bar) and the laser polarization direction are indicated.

polarization causes a corresponding rotation of the ripple pattern. There is a mean ripple spacing of about $\lambda/1.7$; there is also a range of spatial frequencies about this mean value and there is no apparent long-range order. Films grown under somewhat different conditions show mean ripple spacings of from $\lambda/1.2$ to $\lambda/1.7$.

SEM studies of the temporal development of the films have demonstrated the existence of a number of growth stages. Ripple structure occurs only after an initial latency period during which growth in the central region proceeds to a thickness clearly visible by SEM (> 100 nm). The ripple pattern oriented perpendicular to the laser polarization then appears in the central region and spreads radially into the wings of the laser spot. Finally, at later stages of growth, the weaker ripple pattern, oriented parallel to the laser polarization, emerges. SEM observations also clearly distinguish this extensive rippling from fringes resulting from dipole scattering in the vicinity of isolated surface irregularities. These dipolar scattering fringes are highly localized and oriented predominantly parallel to the laser polarization direction.

A series of observations indicate that the ripple structure is associated directly with adsorbed-layer photolysis. Similar ripple structure could not be produced by UV laser irradiation during conventional Cd, Zn, or Al vacuum evaporations, although care was taken to reproduce the film growth rates and laser power densities of the photodeposition process. Photodeposition experiments were also performed at higher pressures (10–20 Torr), where homogeneous gas-phase photolysis governs the film growth rate; under these conditions, the ripples were either much less pronounced or entirely absent. A detailed description of the experimental results will be

published separately.⁷

A number of possible explanations for the film structure have been considered, including interference fringes due to reflections, wave-front aberrations imposed⁵ on the incident laser beam, and dipolar scattering from prominent surface asperities. Each of these may be ruled out by the high spatial frequency or polarization dependence of the ripple.

We have been led to consider the possibility that the rippling arises from the interference between the incident field and the longitudinal electric field component of a SPW launched because of an initial random film granularity. For normal incidence, this interference pattern has the spatial period of the SPW. Since the film growth rate is proportional to the local field intensity, this induces a further growth of the surface profile at the SPW spatial frequency which in turn increases the coupling to the SPW and the strength of the interference pattern.

The small-signal gain coefficient for this process may be evaluated by linearizing the problem and solving for the SPW field intensity with the assumption that the incident field distribution is unchanged by the SPW. For a normal incidence geometry, with the assumption of an isotropic surface roughness distribution, the SPW consists of two equal components oppositely propagating in the incident E -field polarization direction; the extension to oblique angles of incidence will be considered briefly below. With an incident field $\vec{\mathcal{E}}_i = \text{Re}\{E_i \hat{e}_x \exp[-i(\omega t + k_0 z)]\}$ propagating in the $-z$ direction and polarized in the x direction, coupled with a surface grating pattern given by $z_g = u \cos(gx)$ where the medium for $z < z_g$ is a metal of dielectric constant $\epsilon = \epsilon_1 + i\epsilon_2$, and for $z > z_g$ is the organometallic gas of dielectric constant 1, the result^{4,8} for the SPW electric field distribution ($z > z_g$) is

$$\vec{\mathcal{E}}_{sp} = \text{Re} \frac{2uk_g \gamma_g (1 - \epsilon) E_i}{(\gamma_g + \epsilon k_g)(1 + i\Gamma_0/k_0)} [\hat{e}_x \cos(gx) - \hat{e}_z (g/k_g) \sin(gx)] e^{-i\omega t} e^{-k_g z}. \quad (1)$$

Here

$$k_0 = \omega/c; \quad k_g = (g^2 - k_0^2)^{1/2} \quad (\text{Re}k_g > 0); \quad \gamma_g = (g^2 - \epsilon k_0^2)^{1/2} \quad (\text{Re}\gamma_g > 0);$$

and

$$\Gamma_0 = k_0 \sqrt{-\epsilon} \quad (\text{Re}\Gamma_0 > 0).$$

This equation combined with the linear relationship between the film growth rate and the local intensity, $dT/dt = aI(x)$, forms a pair of coupled equations for the grating depth, u , and the SPW field strength, $\vec{\mathcal{E}}_{sp}$. For an assumed spatial pro-

file of $T(x) = T_0 + u \cos(gx)$, the result,

$$\frac{du}{dt} = 8aI_i \text{Re} \left(\frac{k_g \gamma_g (1 - \epsilon)}{(\gamma_g + \epsilon k_g)(1 + |\Gamma_0/k_0|^2)} \right) u, \quad (2)$$

where only the terms up to first order in u have been retained, follows immediately. Both incident and reflected (zero-order) field strengths

have been used in deriving this result. It is instructive to note some of the features of Eq. (2). One of the terms in the denominator, $\gamma_g + \epsilon k_g$, vanishes at the SPW resonance wave vector $\{k_{sp} = [\epsilon_1/(\epsilon_1 + 1)]^{1/2}\}$ for a lossless metal film ($\epsilon_2 \rightarrow 0$). For a real film, loss terms dampen and broaden out the resonance. It is straightforward to show that the resulting intensity modulation is in phase with the surface grating structure for $k_0 \leq g \leq k_{sp}$, independent of ϵ_2 . Thus, there is always a range of spatial wave vectors for which Eq. (2) predicts an exponential growth of the surface structure. Also note that, in analogy with the well-known field divergence at sharp metal points, δ_{sp} increases proportionately to g for $g \gg |\epsilon|k_0$. However, for these high spatial frequencies, du/dt is negative and leads to an exponentially damped grating amplitude.

Before attempting to apply this model to the present experiments, it is necessary to evaluate the SPW parameters which are determined by the average Cd film optical characteristics; these are highly dependent on film thickness and variations in grain size due to growth conditions, surface and vacuum cleanliness, etc.⁹ In the absence of detailed measurements we use the Maxwell-Garnett theory of granular metal films^{9,10} in which the effective ϵ of a composite material composed of spherical dielectric grains with spatial dimensions less than a wavelength, interspersed throughout a metal continuum, is evaluated in terms of the optical properties of the metal and dielectric components with the dielectric volume fraction as the only adjustable parameter. The result is

$$\epsilon_{film} = \frac{\epsilon[2\epsilon(1-X) + (1+2X)]}{[\epsilon(2+X) + (1-X)]}, \quad (3)$$

where X is the insulator volume fraction and the insulator dielectric constant has been taken as unity. We take $\epsilon = -2.5 + i1.3$, as reported¹¹ for the best evaporated Cd films at the UV frequency of the experiment; significant variations are seen for other high-quality vacuum-deposited Cd films.¹² These variations correspond to using the above value for ϵ in Eq. (3) with insulator volume fractions of 0.05–0.10.

Figure 2 shows the calculated growth rates for surface grating structures of spatial wave vector g/k_0 with the insulator volume fraction as a parameter. The absolute growth rate was evaluated from the measured overall film growth rate, $dT_0/dt = aI_i$, of 0.7 nm/s. Also shown in the figure is the growth rate for an idealized metal film with a di-

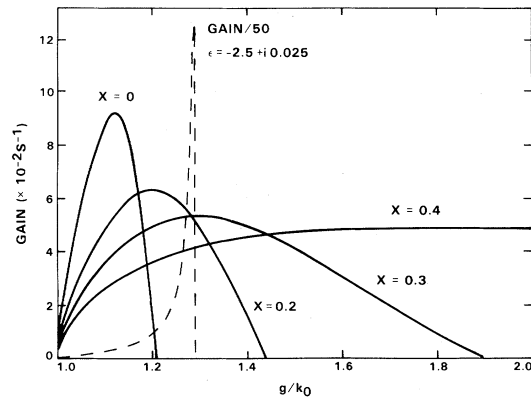


FIG. 2. Calculated growth rates for surface grating structures of spatial wave vector g/k_0 . The dashed curve is for an idealized low-loss metal film. The solid curves are for granular Cd films where X is the volume fraction of voids.

electric constant of $\epsilon = -2.5 + i0.025$. For this almost lossless metal film, the growth rate peaks up sharply just below the SPW wave vector ($k_{sp} = 1.29k_0$). The addition of loss (curve for $X = 0$) greatly broadens and lowers the gain curve. The gain region shifts to higher spatial wave vectors as the insulator volume fraction is increased because of the decreasing resonance frequency in the composite films.¹⁰ For $X = 0.4$ the gain curve peaks at $g/k_0 \sim 1.6$ and shows substantially the same gain over the region $1.2 < g/k_0 < 3$. This is consistent with the observed variation in spatial frequencies of the deposited surface structures seen in Fig. 1. For other deposition conditions, somewhat lower-insulator-content metal films with gain profiles peaking closer to $1.2k_0$ are formed. These films have grating structures with a narrower range of spatial wave vectors. The absolute gain coefficients are sufficiently large to explain the growth of film grating structures from scale sizes of 1–10 nm to the observed scales of ~ 100 nm during the 300-s growth times of a typical experiment. A distribution of surface roughness on this scale is virtually guaranteed by the granular nature of the films. There is also a self-limiting effect: As u becomes comparable to λ , the surface profile substantially modifies the SPW dispersion characteristics¹³ and the SPW coupling saturates and becomes independent of u . The simple model presented here does not treat these effects which may modify the final surface profiles.

For oblique angles of incidence with the field polarized in the plane of incidence (p polarization), the surface grating profiles that allow the

incident wave to couple to the two oppositely propagating SPW waves are no longer degenerate. The two spatial wave vectors are $g_0 \pm k_0 \sin\theta$ where g_0 is the peak g for normal incidence. The interference patterns show the same spatial period and again there are regions of exponential growth. For s polarization, the results for normal incidence are unchanged. These results are consistent with the observed spatial patterns in films grown at oblique incidence. Once this dominant surface grating is established, there is a weak coupling into a SPW traveling in the orthogonal direction (e_y) due to non-normal angles of incidence.^{4,8} This SPW may be responsible for the weaker observed spatial structure; the coupling depends on the depth of the initial surface grating and does not lead to exponential growth.

We have described a new nonlinear optical effect in which the coupling of incoming radiation to surface plasma waves leads to an exponential growth of a periodic film structure during film growth by UV photodeposition. These interactions may ultimately be useful in directly growing periodic solid-state device structures on a UV-wavelength spatial scale. Grating surface structure has also been observed in laser-annealed Si and Ge samples.¹⁴ The structure shows the same polarization and angle-of-incidence characteristics as the ripple structure reported here. There is no SPW supported at a Si/air interface for typical laser wavelengths of 0.5–1 μm . However, the necessary conditions for a SPW are satisfied for a liquid-Si/air interface and evaluation of Eq. (2) for liquid Si optical constants¹⁵ gives a narrow region of in-phase coupling extending through $1.0 < g/k_0 < 1.01$ which would explain the high degree of long-range order observed in these laser-an-

nealed gratings.

We would like to thank R. M. Osgood, Jr., for making important contributions to the understanding of this problem, and to acknowledge the important technical contribution of D. J. Sullivan. We also wish to thank P. L. Kelley, D. L. Mills, J. E. Sipe, and J. Y. Tsao for helpful discussions. This work was supported by the U. S. Department of the Army and the U. S. Department of the Air Force.

¹R. H. Ritchie, *Surf. Sci.* **34**, 1 (1973).

²R. W. Wood, *Philos. Mag.* **4**, 396 (1902).

³C. K. Chen, A. R. B. de Castro, Y. R. Shen, and F. DeMartini, *Phys. Rev. Lett.* **43**, 946 (1979).

⁴S. S. Jha, J. R. Kirtley, and J. C. Tsang, *Phys. Rev. B* **22**, 3973 (1980).

⁵D. J. Ehrlich, R. M. Osgood, Jr., and T. F. Deutsch, *IEEE J. Quantum Electron.* **16**, 1233 (1980).

⁶D. J. Ehrlich and R. M. Osgood, Jr., *Chem. Phys. Lett.* **79**, 381 (1981).

⁷R. M. Osgood, Jr. and D. J. Ehrlich, to be published.

⁸A. Marvin, F. Toigo, and V. Celli, *Phys. Rev. B* **11**, 2777 (1975).

⁹O. S. Heavens, *Optical Properties of Thin Solid Films* (Dover, New York, 1965), pp. 39–42.

¹⁰J. P. Marton and J. R. Lemon, *Phys. Rev. B* **4**, 271 (1971).

¹¹T. M. Jelinek, R. N. Hamm, E. T. Arakawa, and R. H. Huebner, *J. Opt. Soc. Am.* **56**, 185 (1966).

¹²S. Robin-Kandare, J. Robin, and S. Kandare, *J. Phys. (Paris)* **25**, 218 (1964).

¹³I. Pockrand, *J. Phys. D* **9**, 2423 (1976).

¹⁴D. C. Emmony, R. P. Howson, and L. J. Willis, *Appl. Phys. Lett.* **23**, 598 (1973).

¹⁵K. M. Shvarev, B. A. Baum, and P. V. Gel'd, *Fiz. Tverd. Tela* **16**, 3246 (1974) [*Sov. Phys. Solid State* **16**, 2111 (1975)].

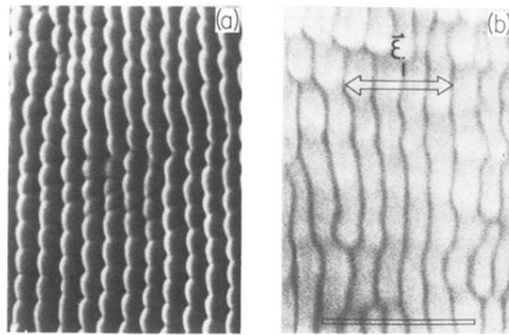


FIG. 1. SEM's of ripple structure in a ~ 200 -nm-thick photodeposited Cd film on a SiO_2 substrate at viewing angles of (a) 60° , and (b) normal incidence. A $1\text{-}\mu\text{m}$ scale (horizontal bar) and the laser polarization direction are indicated.